EurJOC
European Journal
of Organic Chemistry

FULL PAPER

Matrix Isolation and Spectroscopic Characterization of 2,5,6-Trifluoropyridylnitren-3-yl

## Dirk Grote,[a] Christopher Finke,[a] Patrik Neuhaus,[a] and Wolfram Sander*[a]

The photochemistry of 3-iodo-2,5,6-trifluoropyridyl azide (**6c**), matrix-isolated in argon, was investigated by IR and EPR spectroscopy. The primary photoproduct is 3-iodo-2,5,6-trifluoropyridylnitrene (**7c**) in its triplet ground state. Further irradiation produced very low yields of nitrene radical **3c**, which shows a characteristic EPR spectrum. The yield of **3c**, however, was too low for IR detection. Instead, azirinyl radical **11**, formed from **3c** by ring closure, could clearly be identified in the IR spectra. Other products observed were azirine **8c′** and the ketenimine **9c′**, which are formed in a photostationary equilibrium together with nitrine **7c**.

Introduction

High-spin molecules are the basis for the development of organic magnets and are intensively studied in many laboratories throughout the world.[1] A common motif used to stabilize high-spin states are π radical centers coupled by a *meta*-phenylene unit such as in *m*-xylylene **1** with a triplet ground state[2] or trimethylenebenzene **2** with a quartet ground state.[3] The *meta*-phenylene unit has proven to be a robust coupling unit to achieve ferromagnetic coupling between π radical centers.[4]
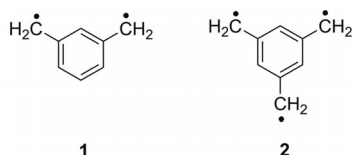
A different approach to molecules with high-spin ground states is the combination of π and σ radical centers.[5] Ab-initio and DFT calculations suggest that *ortho*- and *para*-nitrene radicals **3** and **5** have a high-spin quartet ground state, whereas *meta*-nitrene radical **4** is a doublet ground state molecule.[6] This has been confirmed by matrix isolation studies of several derivatives of **3** and **5**, which all show quartet ground states.[1a,7] Attempts to synthesize derivatives of **4** failed, and only ring-opened products were observed.[8] The electronic structure of **3** and **5** can be described as σ,σ,π triradicals resembling both nitrenes and carbenes, as shown in the resonance structures below. The carbene character of nitrene radicals **3** and **5** results in un-

usually large zero field splitting (zfs) parameters E in these molecules, in accordance with quantum-chemical calculations.[1a,7c]
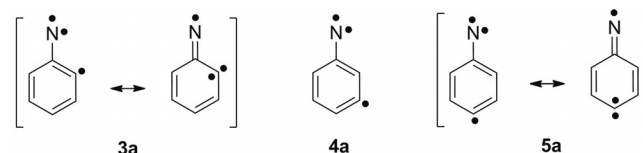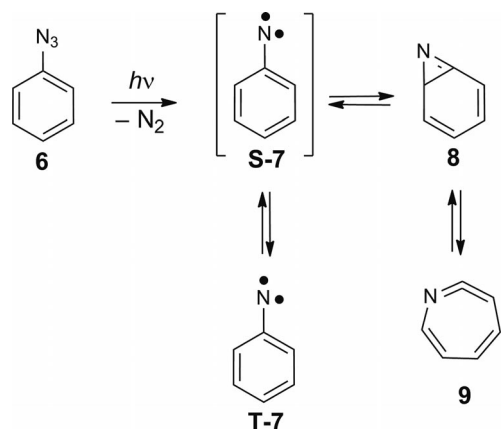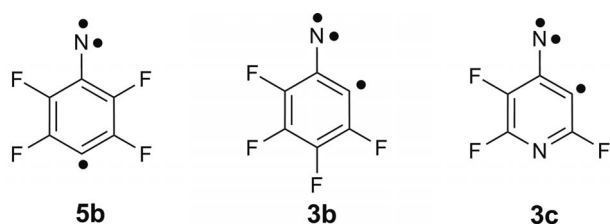

Precursors of nitrene radicals **3–5** are iodophenyl azides, which, on photolysis, split off N_2 to give phenyl nitrenes as primary photoproducts. In a second step, requiring prolonged photolysis, the C–I bond is cleaved to produce the corresponding nitrene radicals. Unwanted side reactions reducing the yields of phenyl nitrenes are the photochemical rearrangements to azirines **8** and ketenimines **9**. These rearrangements have been extensively studied over the last decades.[9] During the photolyis of phenyl azides, phenyl nitrenes **7**, azirines **8**, and ketenimines **9** are formed in photostationary equilibria with yields that depend on the irradiation conditions (Scheme 1).[9a]

Fluorine substituents in the *ortho* position of the aromatic ring raise the barriers for these rearrangements,[10] and thus fluorinated phenylnitrenes are formed in higher yields. Because the efficiency of cleavage of the C–I bonds in an inert matrix is low due to in-cage recombinations, the only nitrene radicals that could be isolated in a matrix so far bear at least one fluorine substituent in the *ortho* position.[1a,7]

2,3,5,6-Tetrafluorophenylnitren-4-yl (**5b**) was the first nitrene radical that could be matrix-isolated and characterized as a quartet ground state molecule by IR and EPR spectroscopy.[1a,7a] In the following years, several phenylnitren-4-yl compounds with a large variety of fluorine substitution were synthesized and characterized by IR and EPR spectroscopy.[7b]

[a] Lehrstuhl für Organische Chemie II, Ruhr-Universität Bochum,
44780 Bochum, Germany
Fax: +49-234-321-4353
E-mail: wolfram.sander@rub.de
Supporting information for this article is available on the WWW under http://dx.doi.org/10.1002/ejoc.201101866.

© 0000 Wiley-VCH Verlag GmbH & Co. KGaA, Weinheim

WILEY
ONLINE LIBRARY

FULL PAPER

D. Grote, C. Finke, P. Neuhaus, W. Sander

Scheme 1. Photochemistry of phenyl azide **6**.

Recently, we reported on the matrix isolation and EPR spectroscopic characterization of the first *ortho* nitrene radical 3,4,5,6-tetrafluorophenylnitren-2-yl (**3b**).[7c] The EPR spectrum of **3b** clearly corroborates a quartet ground state for this nitrene radical. By the less selective and less sensitive IR spectroscopic analysis, however, **3b** could not be detected. Instead, the thermodynamically more stable rearranged azirinyl radical **10** was found (Scheme 2). Because **10** is a radical with a doublet ground state, whereas **3b** has a quartet ground state, the ring closure of **3b** requires a spin inversion. This should result in an activation barrier of at least the magnitude of the doublet–quartet gap of **3b**, calculated to be 7.0 kcal/mol, and thus not occur thermally in

low temperature matrices. For this reason, it was concluded that the ring closure of **3b** is a photochemical rather than thermal reaction.[7c] Other products formed during the photolysis of **6b** were the azirines **8b** and **8b′** and the ketenimines **9b** and **9b′** (Scheme 2).

Substitution of a CF group in **3b** by a nitrogen atom results in a heterocyclic nitrene radical. These unique triradicals would allow us to study the influence of a nitrogen atom on the spin distribution in nitrene radicals and, in particular, determine whether these systems still maintain a high-spin ground state. Here, we report on the matrix isolation and spectroscopic characterization of the first pyridylnitrene radical.

Results

UV Irradiation ($\lambda = 254$ nm) of an argon matrix (16 K) doped with small amounts of 3-iodo-4,5,6-trifluoropyridyl azide (**6c**) results in a rapid decrease of the IR bands of **6c** and a rapid increase of newly formed strong absorptions at 1572, 1487, and 1395 cm^{-1}. By comparison with the IR spectrum calculated at the (U)B3LYP/6-311G(d,p) level of theory, these bands could be assigned to triplet 3-iodo-2,5,6-trifluoropyridylnitrene **T-7c** (Table 1, Figure 1). The calculated IR spectrum is in reasonable agreement with the experimental spectrum. At short irradiation times, **7c** is the only detectable photoproduct.

Upon further irradiation with UV light of 254 nm, a new set of IR absorptions at 1586, 1559, and 1276 cm^{-1} is formed, while the bands assigned to triplet nitrene **7c** concurrently decreased. The absorption at 1831 cm^{-1} is characteristic of the cumulene C=C=N st. vibration of ketenimines.[7b,7c,9b,11] Detailed investigation of the IR spectrum revealed that only one of the two possible ketenimines **9c′** is formed. No trace of the isomeric ketenimine **9c** was observed in the matrix (Figure 2, Table 2).

The IR spectrum revealed additional bands that formed simultaneously with the absorptions of the ketenimine. A
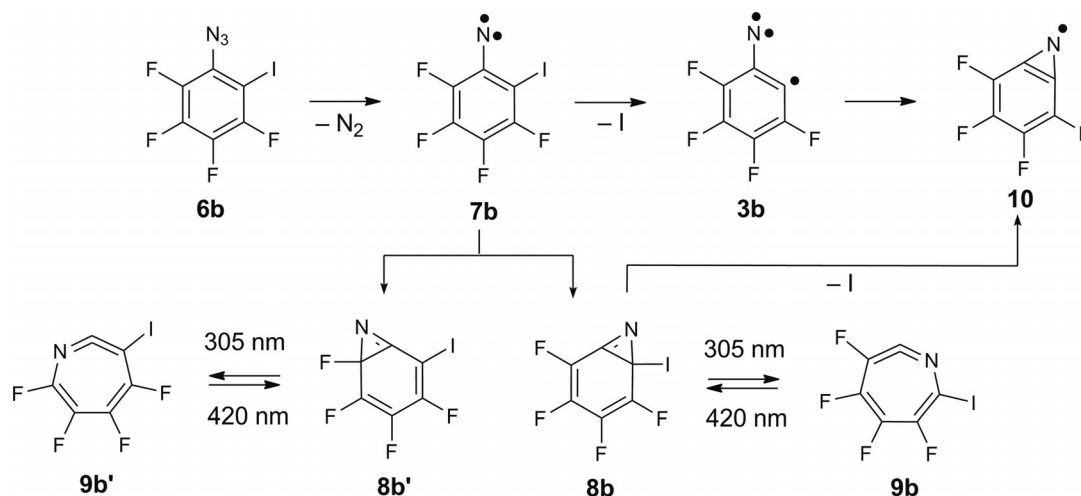

Scheme 2. Photochemistry of aryl azide **6b**.

Isolation and Characterization of 2,5,6-Trifluoropyridylnitren-3-yl

EurJOC
European Journal
of Organic Chemistry

Table 1. IR spectroscopic data of 3-iodo-2,5,6-trifluoropyridyl-nitrene (**7c**).

Mode	Symm.	$\tilde{\nu}_{exp.}$ [cm^{-1}][a]	$I_{rel., exp.}$[a,b]	$\tilde{\nu}_{calcd.}$ [cm^{-1}][c]	$I_{rel., calc}$[b,c]
14	A′	614.2	0.03	612.8	0.01
16	A′	686.3	0.04	694.2	0.01
17	A″	723.0	0.03	724.2	0.02
18	A′	830.8	0.23	831.7	0.22
19	A′	1048.4	0.11	1057.9	0.13
20	A′	1098.3	0.23	1113.8	0.14
21	A′	1220.5[d]	—[d]	1223.5	0.05
22	A′	1266.8[d]	—[d]	1260.2	0.48
23	A′	1275.7[d]	—[d]	1282.3	0.24
24	A′	1381.3	0.08	1403.5	1.00
		1385.0	0.14		
25	A′	1395.3	1.00	1415.5	0.53
26	A′	1487.0	0.76	1528.0	0.46
27	A′	1571.5	0.95	1591.6	0.54

[a] Ar, 3 K. [b] Band intensity relative to the strongest absorption. [c] UB3LYP/6-311G(d,p), unscaled. [d] Assignment tentative due to some deviations in intensity and band positions between experimental and calculated spectrum probably caused by Fermi resonance.
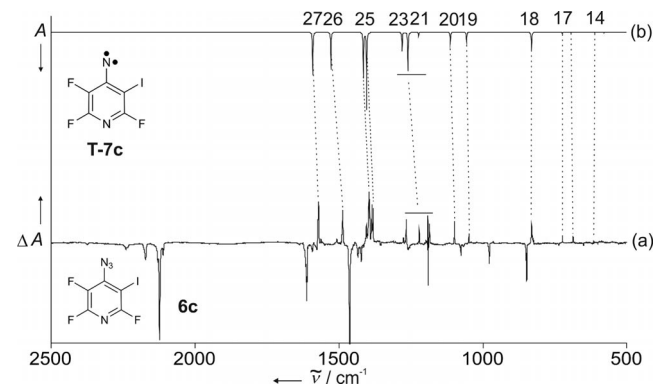

Figure 1. IR spectra showing the 254 nm photochemistry of azide **6c** in argon at 10 K after 1 min irradiation. (a) Difference IR spectrum: Bands of **6c** pointing downwards disappear and bands of triplet pyridylnitrene **T-7c** pointing upwards appear during irradiation. (b) IR spectrum of **T-7c** calculated at the UB3LYP/6-311G(d,p) level of theory (vibrational modes 14 to 27, see Table 1).

strong band appeared at 1450 cm^{-1}, and some weaker bands at 1366, 1102, 953, and 818 cm^{-1}. These bands increased upon subsequent UV irradiation, whereas bands assigned to pyridyl nitrene decreased. After 3.5 h irradiation at 254 nm, the newly formed species was the final photoproduct found in the matrix (Figure 3). By comparison with UB3LYP/6-311G(d,p) calculations (Table 3) the newly formed compound was assigned to azirinyl radical **11**. According to DFT calculations, radical **11** is 15.5 kcal/mol more stable than quartet nitrene radical **Q-3c**.

Irradiation of the matrix containing ketenimine **9c′** with visible light (λ = 450 nm) yields new IR signals at 1509, 1359, 1304, and 1201 cm^{-1}, while the bands assigned to **9c′** decrease at the same time (Figure 4, Table 4). By comparison with absorptions calculated at the B3LYP/6-311G(d,p) level of theory, the new bands are assigned to azirine **8c′**. The isomeric azirine **8c** was not found in the matrix. The band of **8c′** calculated at 1620 cm^{-1} was not observed in
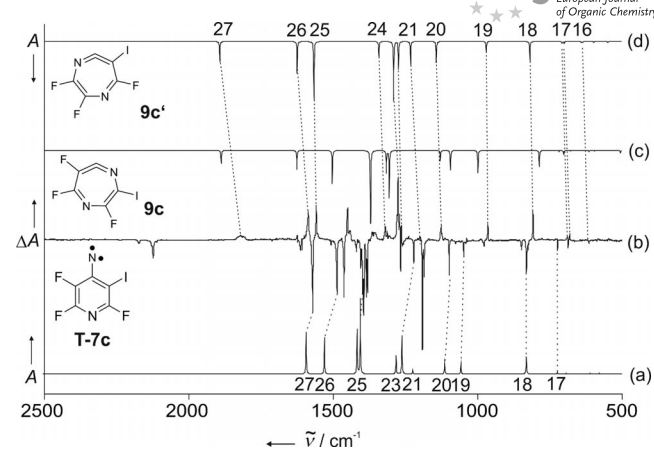

Figure 2. IR spectra showing the photochemistry of nitrene **T-7c** after 5 min irradiation at 254 nm (argon, 10 K). (a) Calculated spectrum of nitrene **T-7c** (vibrational modes 17 to 27, see Table 1). (b) Difference IR spectrum: Bands of **T-7c** pointing downwards disappear and bands of ketenimine **9c′** pointing upwards appear during irradiation. (c) Calculated IR spectrum of **9c′**. (d) Calculated spectrum of **9c** (vibrational modes 16 to 27, see Table 2). All calculations at the (U)B3LYP/6-311G(d,p) level of theory.

Table 2. IR spectroscopic data of ketenimine **9c′**.

Mode	$\tilde{\nu}_{exp.}$ [cm^{-1}][a]	$I_{rel., exp.}$[a,b]	$\tilde{\nu}_{calcd.}$ [cm^{-1}][c]	$I_{rel., calc}$[b,c]
16	681.0	0.13	700.3	0.04
17	689.3	0.09	708.9	0.04
18	808.4	0.46	819.6	0.33
19	964.2	0.36	970.2	0.18
20	1125.9	0.66	1143.5	0.35
21	1198.7	0.63	1232.6	0.39
22	1264.5	0.21	1274.9	0.46
23	1275.9	1.00	1291.9	1.00
24	1320.4	0.25	1342.9	0.27
25	1558.7	0.71	1566.9	0.97
26	1586.3	0.70	1624.9	0.53
27	1830.6	0.04	1893.3	0.35

[a] Ar matrix, 3 K. [b] Relative Intensity based on the strongest absorption. [c] B3LYP/6-311G(d,p), unscaled.
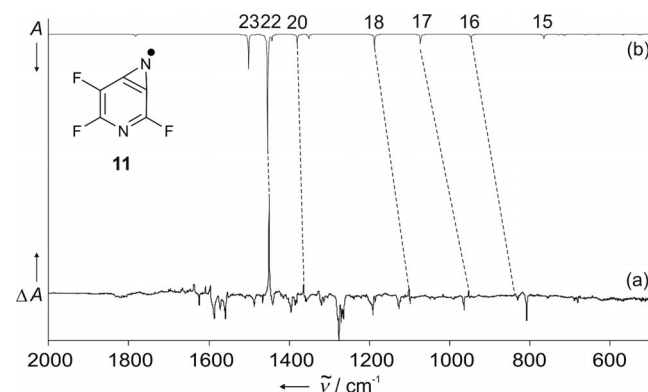

Figure 3. IR spectra showing the photochemistry of azide **6c** (3.5 h irradiation at 254 nm, argon, 3 K). (a) Difference IR spectrum: Bands pointing upwards assigned to **11** appear, and bands pointing downwards disappear during irradiation. (b) IR spectrum of **11** calculated at the UB3LYP/6-311G(d,p) level of theory (vibrational modes 15 to 23, see Table 3).

FULL PAPER

D. Grote, C. Finke, P. Neuhaus, W. Sander

Table 3. IR spectroscopic data of azirinyl radical **11**.

Mode	Symm.	$\tilde{v}_{exp.}$ [cm^{-1}][a]	$I_{rel., exp.}$[a,b]	$\tilde{v}_{calcd.}$ [cm^{-1}][c]	$I_{rel., calc}$[b,c]
13	A″	–	–	715.4	0.01
14	A′	–	–	724.5	0.01
15	A′	644.8	0.05	763.9	0.04
16	A′	817.5	0.12	945.2	0.04
17	A′	952.8	0.13	1075.4	0.08
18	A′	1101.9	0.35	1191.4	0.12
19	A′	–	–	1353.8	0.03
20	A′	1365.9	0.33	1390.7	0.08
21	A′	–	–	1444.9	0.08
22	A′	1450.4	1.00	1465.0	1.00
23	A′	–	–	1506.4	0.36
24	A′	–	–	1784.8	0.02

[a] Argon matrix, 3 K. [b] Relative intensity based on the strongest absorption. [c] UB3LYP/6-311G(d,p), unscaled.

Table 4. IR spectroscopic data of azirine **8c′**.

Mode	$\tilde{v}_{exp.}$ [cm^{-1}][a]	$I_{rel., exp.}$[a,b]	$\tilde{v}_{calcd.}$ [cm^{-1}][c]	$I_{rel., calc}$[b,c]
15	683.0	0.08	701.7	0.03
16	693.5	0.07	715.1	0.03
17	753.3	0.37	764.1	0.08
18	881.3	0.24	891.5	0.09
19	1018.2	0.48	1029.3	0.09
20	–	–	1081.2	0.10
21	–	–	1121.4	0.11
22	1200.5	0.41	1200.7	0.24
23	1303.8	0.54	1333.0	0.36
24	1359.0	1.00	1368.3	1.00
25	1508.9	0.44	1525.1	0.38
26	–	–	1620.4	0.44
27	–	–	1774.4	0.08

[a] Argon matrix, 3 K. [b] Relative intensities based on the strongest absorption. [c] B3LYP/6-311G(d,p), unscaled.

the difference spectrum because it overlaps with a broad absorption of ketenimine **9c′** at 1586 cm^{-1}. UV irradiation of **8c′** yields ketenimine **9c′** and the azirinyl radical **11**.
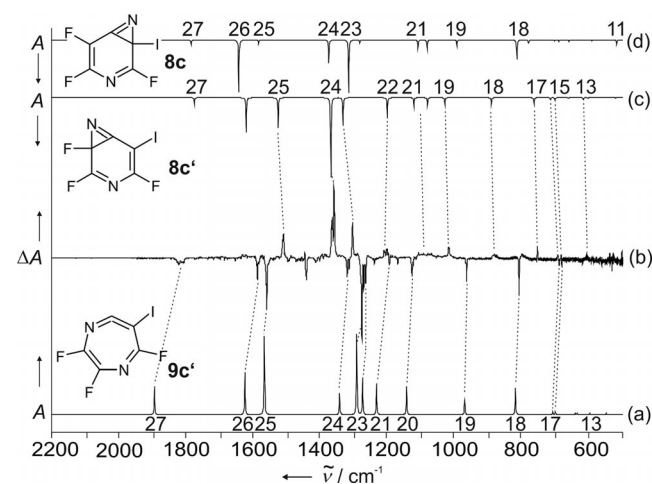

Figure 4. IR spectra showing the 450 nm photochemistry of ketenimine **9c′** in argon at 3 K after 10 seconds irradiation with visible light (λ = 450 nm). (a) Calculated spectrum of ketenimine **9c′** (vibrational modes 13 to 27, see Table 2). (b) Difference IR spectrum: Bands of **9c′** pointing downwards disappear and bands of azirine **8c′** pointing upwards appear during irradiation. No traces of **8c** were found in the matrix. (c) Calculated IR spectrum of **8c** (vibrational modes 13 to 27, see Table 4); (d) Calculated IR spectrum of **8c′** (vibrational modes 11 to 27). All calculations at the B3LYP/6-311G(d,p) level of theory.

To detect the paramagnetic species formed during the photolysis of **6c**, EPR spectra of the photoproducts were recorded in argon at 5 K. A set of very weak signals characteristic of a quartet species with ZFS parameters |D/hc| = 0.384 cm^{-1} and |E/hc| = 0.0088 cm^{-1} (g = 2.003, v = 9.60883 GHz) suggests the formation of quartet nitrene radical **3c**. By solving the spin Hamiltonian for the orientation of the quartet spin system parallel to the axes x and y, the EPR signals were assigned to the transitions y1, x1, x3, and y3 (see Figures 5, 6).

Two EPR transitions at 6240 and 6500 G cannot be assigned to the canonical orientations. These "off-axis" transitions (labeled "A" in Figure 6) are higher order solutions
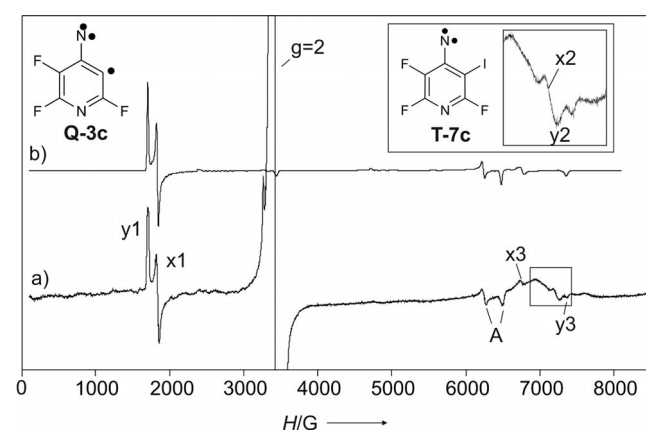

Figure 5. EPR spectra showing the photochemistry of pyridyl nitrene **T-7c**. (a) EPR spectrum after UV irradiation (argon, 5 K) of azide **6c**. The signals x2 and y2 are assigned to nitrene **T-7c** with a D value of |D/hc| = 1.110 cm^{-1} (g = 2.003, v = 9.60883 GHz). A very strong signal at g = 2 indicates the formation of radical species. (b) Simulated spectrum of quartet nitrene radical **Q-3c** with ZFS parameters |D/hc| = 0.384 cm^{-1} and |E/hc| = 0.0088 cm^{-1} (g = 2.003, v = 9.60883 GHz).

of the spin Hamiltonian, and are typical of EPR spectra of high-spin systems with S > 3/2. These transitions are assigned to orientations of about 25° in the zx plane and 30° in the zy plane (Figure 7). Transitions parallel to z are weak and were not observable in the experimental spectrum under these conditions. Figure 7 also shows the slightly off-axis behavior of transition z4,[1a] which becomes allowed if the z axis is rotated slightly away from the direction of the magnetic field.[12]

The EPR signals of **3c** disappear upon annealing of the matrix at 30 K, which is typical of matrix-isolated radical pairs that recombine at temperatures at which the matrix becomes soft, and trapped species are able to diffuse rapidly. If the matrix is cooled back to 5 K and irradiated with UV light, the signals of **3c** appear again.

In addition to the signals of **3c**, the EPR spectrum shows very weak x2 and y2 transitions of a triplet system, assigned to nitrene **T-7c**. By simulating a triplet species with a D
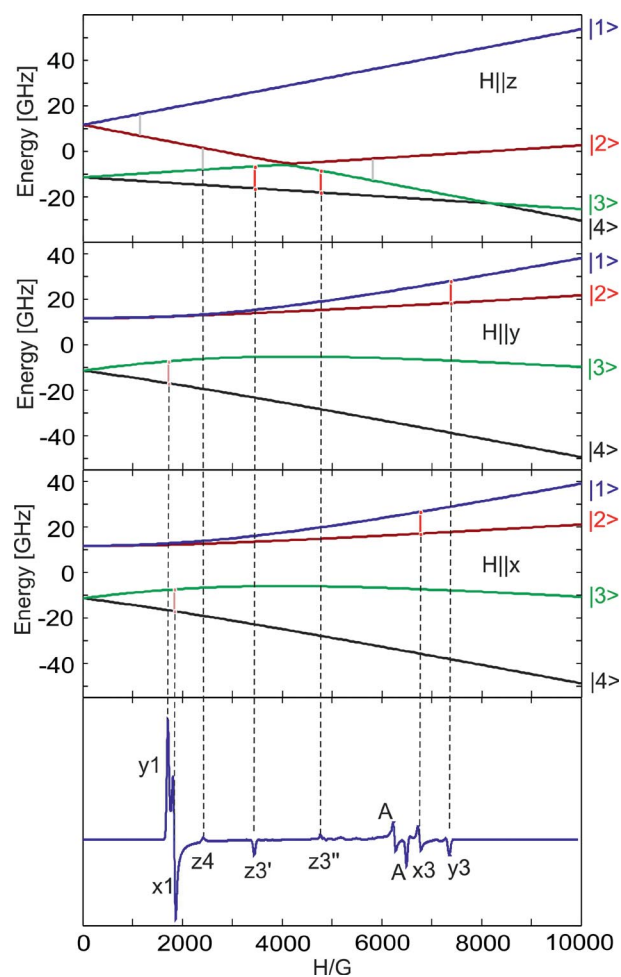
Isolation and Characterization of 2,5,6-Trifluoropyridylnitren-3-yl

Figure 6. The four sublevels of quartet **Q-3c** with the external field H parallel to the z, x, and y-axis, respectively, calculated using the ZFS parameters $|D/hc| = 0.384$ cm^{-1}, $|E/hc| = 0.0088$ cm^{-1} ($g = 2.003$).
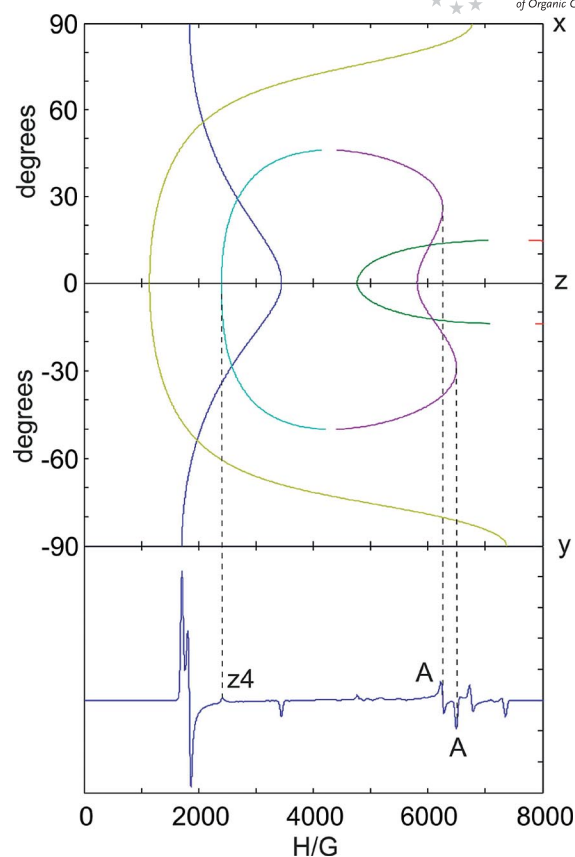

Figure 7. Angular dependence of the EPR signals of **Q-3c** when varying the field orientation from parallel to x to parallel to z and parallel to y. The signals A are assigned to off-axis transitions. The plot also shows the slightly off-axis behavior of transition z4.

value of $|D/hc| = 1.110$ cm^{-1} ($g = 2.003$, $v = 9.60883$ GHz), the spectrum of **T-7c** is reproduced. Due to the low signal intensity and overlap with the quartet signals, the simulation is only tentative and no reliable E value could be derived. A very strong doublet signal appears at $g = 2$, indicating that radicals are formed as the final products of the UV irradiation. Due to the lack of resolved hyperfine splitting, the radicals could not be assigned.

Discussion

Photochemsitry of 7c

The photochemistry of **7c** is quite similar to that of 2-iodo-3,4,5,6-tetrafluorophenyl azide (**7b**) described previously.[7c] Upon irradiation with UV light, triplet nitrene **T-7c** is the first photoproduct formed. Subsequent UV irradiation results in the formation of ketenimine **9c′**, which is formed through ring opening of azirine **8c′**. When the matrix is irradiated with visible light ($\lambda = 420$ nm), azirine **8c′** is produced in yields high enough for IR detection in a

photostationary equilibrium with **7c** and **9c′**. The isomeric azirine **8c** and ketenimine **9c** are not observed under these conditions, which indicates that the rearrangement of **7c** is highly selective (Scheme 3). The same type of selectivity, although less pronounced, was previously found for the rearrangement of **7b**, for which **8b** and **9b** were the minor products (Scheme 2).[7c]

The photochemical rearrangement of triplet **7c** to the singlet products **8c′** and **9c′** involves an intersystem crossing step from the triplet to the singlet surface. Although the rearrangement of **7c** is induced by light, we cannot discriminate true photochemical reactions from "hot" ground state reactions. Presumably, the irradiation of **T-7c** results in the formation of vibrationally excited **S-7c**, which subsequently rearranges to **8c′** and **9c′**.

To gain insight into the mechanisms of these rearrangements, we compared the calculated energies and activation barriers of **7c** and its photoproducts (Figure 8) and found that **8c′** is 6.6 kcal/mol more stable than **8c**. The barriers for the formation of **8c** and **8c′** are 27.6 and 24.9 kcal/mol, respectively, and thus the thermodynamically preferred azirine **8c′** is also kinetically preferred by 2.7 kcal/mol. Similar correlations were observed for a large number of substituted phenylnitrenes.[7b,7c] In all cases the preferred pho-

D. Grote, C. Finke, P. Neuhaus, W. Sander
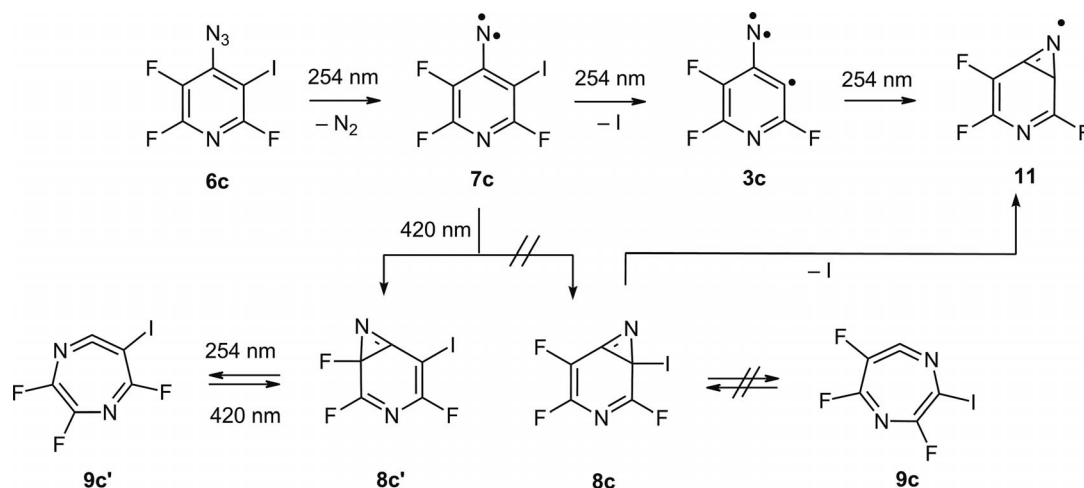
Scheme 3. Photochemistry of 3-iodo-2,5,6-trifluoropyridyl azide (**6c**) in argon or neon matrix.

toproduct depends on the relative stabilities of the formed azirines and ketenimines, as well as on the activation barriers for the formation of azirines.
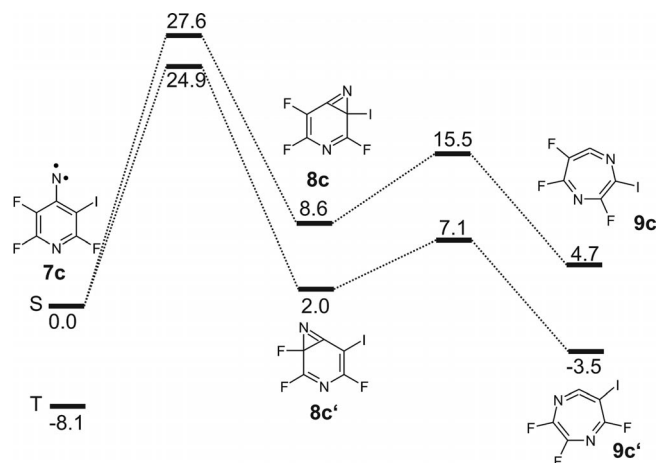

Figure 8. Energies of **7c** and its isomers calculated at the (U)B3LYP/6-311G(d,p) level of theory.

Nitrene Radical

As expected, the primary photoproduct of the photolysis of azide **6c** is pyridyl nitrene **7c**. However, **7c** is formed in lower yields than phenyl nitrene **7b** under comparable conditions from phenyl azide **6b**, indicating the sensitivity of **7c** towards rearrangements to ketenimines and azirines. The EPR spectrum of **7c** exhibits the characteristic pattern and ZFS parameters of a triplet phenylnitrene, similar to that of iodinated phenyl azides investigated previously.[1a,7,8] The xy2 transition is quite broad, indicating a nonzero E value that is smaller than that of **7b** ($|E/hc| = 0.0071$ cm^{-1}). However, because no splitting of the signal was observed, and because the signal overlapped with quartet signals, the E

value could not be determined. Due to the heavy atom effect of iodine, the ZFS parameters of **7b** and **7c** are significantly influenced by spin-orbit coupling (SOC).

Nitrene radical **3c** is formed from nitrene **7c** upon subsequent irradiation with UV light in very low yield. The D value obtained from the EPR spectrum of **3c** by simulation ($|D/hc| = 0.384$ cm^{-1}) is larger than that found for nitrene radical **3b** ($|D/hc| = 0.357$ cm^{-1}), while the E value of **3c** ($|E/hc| = 0.0088$ cm^{-1}) is smaller than that of **3b** ($|E/hc| = 0.0136$ cm^{-1}).

DFT calculations indicate that nitrene radicals such as **3b** and **3c** simultaneously exhibit a nitrene and a carbene character that both contribute to the overall quartet **D** tensor. The magnetic z axis of the nitrene subunit is oriented parallel to the C–N bond, whereas the easy axis of the carbene subunit lies parallel to a hypothetical 180° bond angle at the spin center. The nitrene center, with larger dipolar interactions, dominates the overall spin system, but the dipolar field of the carbene moiety contributes to the y direction perpendicular to the z axis of the nitrene. Thus, the easy axis of the **D** tensor of the quartet spin system of **3b** is rotated about 1° in the molecular plane away from the C–N bond. The carbene contribution in the y direction leads to magnetically nonequivalent x and y axes, which is reflected in the E value of the quartet system. This qualitative description of the magnetic properties can also be applied to **3c**. The difference between **3b** and **3c** is the replacement of a CH group in the aromatic ring by a nitrogen atom in **3c**, which changes the spin distribution in the ring. The spin population at the nitrene center of **3c** is calculated to be 1.64, which is slightly higher than in **3b** (1.60), whereas the spin population at the carbene center is lower in **3c** (1.24) than in **3b** (1.26). This finding is in accordance with the EPR results. A comparison of the EPR spectra reveals that the D value of **3c** is larger than that of **3b**, whereas the E value is smaller. The D value is strongly influenced by the delocalization of the π electron into the aromatic ring. Because this delocalization is smaller in **3c**, due

to the nitrogen atom in the ring, the π electron is more localized at the nitrene center, which results in the larger *D* value of **3c**. The *E* value, in turn, is strongly influenced by the carbene contribution to the overall spin system. This influence is smaller in **3c** because of the lower spin population at the carbene center. The larger spin population at the nitrene center adds to the nitrene contribution exceeding the carbene contribution, resulting in the smaller *E* value in **3c** compared to **3b**.

Azirinyl Radical

Azirinyl radical **11** is most likely formed from nitrene radical **3c** in an excited doublet state by ring closure between the nitrogen atom and the adjacent radical center in the *ortho* position.

At the UB3LYP/6-311G(d,p) level of theory, **11** was calculated to be 14.5 kcal/mol more stable than the nitrene radical **3c**. A similar azirinyl radical **10** was described previously as the final photoproduct of the UV photolysis of azide **6b**.[7c] According to DFT calculations, both azirinyl radicals are planar. With a spin population of 0.62, the azirine nitrogen atom bears the major part of the spin density in the radical. The rest of the spin density is delocalized into the aryl rings of **10** and **11**, respectively (Figure 9).
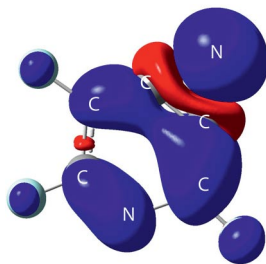

Figure 9. Spin-density distribution of azirinyl radical **11** [UB3LYP/ 6-311G(d,p)], which shows C_s symmetry; the spin density is delocalized into the aromatic π system.

Conclusions

The chemistry of triplet nitrene **7c** and quartet nitrene radical **3c** nicely fits into the general scheme that has been developed for these reactive intermediates. The yields of photochemically generated nitrene radicals such as **7c** is diminished by rearrangements to the corresponding azirines and ketenimines.[7b,7c,8,9] By carefully selecting the irradiation conditions (wavelength and monochromatic vs. broadband source), the yield of the nitrenes can be optimized, but generally remains quite poor. Nitrene radicals with radical centers in the *ortho* or *para* positions with respect to the nitrene unit show quartet ground states, and nitrene radical **3c** is no exception to this rule. The presence of the ring nitrogen atom results in a shift of charge density towards this nitrogen atom, and an increased spin density at the nitrene center, compared to nitrene radical **3b**. The increased spin density at the nitrene center, in turn, results in

a larger *D* value of the quartet system, which can be detected by EPR spectroscopy. The thermodynamic sink for *ortho* nitrene radicals such as **3c** is the formation of a bond between the nitrogen atom and the *ortho* carbon atom to give azirinyl radicals. With radical **11** the second example of these elusive radicals has now be spectroscopically characterized.

Experimental Section

3-Iodo-2,5,6-trifluoropyridyl Azide (6c): Synthesized analogously to 2-iodo-3,4,5,6-tetrafluorophenyl azide[7c] (**6b**). Yield 55%. IR (Ar, 4 K): ṽ (%) = 2120.8 (85), 1506.6 (100), 1481.1 (45), 1405.1 (7), 1283.9 (6), 1252.1 (10), 1119.3 (23), 1065.7 (24), 934.5 (23), 818.8 (22) cm^{-1}. ^{19}F NMR (400 MHz, CDCl$_3$): δ = –56.1 (s), –88.8 (s), –155.9 (s) ppm. ^{13}C NMR (100 MHz, CDCl$_3$): δ = 64.8 (d, J = 50.1 Hz), 136.5 (d, J = 258.1 Hz), 144.6 (s), 149.7 (d, J = 229.4 Hz), 155.3 (d, J = 237.4 Hz) ppm. MS: m/z (%) = 300 (100) [M$^+$], 272 (7) [M$^+$ – N$_2$], 145 (35) [M$^+$ – I – N$_2$], 127 (20) [M$^+$ – N$_2$ – I – F], 76 (10) [M$^+$ – I – N$_3$ – 3F]. C$_5$F$_3$IN$_4$ (302.00): calcd. C 19.8, N 18.5; found C 19.99, N 18.35.

Matrix Isolation: Matrix isolation experiments were performed by using standard techniques[13] with closed-cycle helium cryostats allowing cooling of a CsI spectroscopic window to 4 K. FTIR spectra were recorded with a standard resolution of 0.5 cm^{-1}, using a N$_2$(*l*)-cooled MCT detector in the range 400–4000 cm^{-1}. X-band EPR spectra were recorded with a Bruker Elexsys E500 EPR spectrometer with an ER077R magnet (75 mm pole cap distance), an ER047 XG-T microwave bridge, and an oxygen-free high-conductivity copper rod (75 mm length, 3 mm diameter) cooled by a closed-cycle cryostat.

Broadband irradiation was carried out with mercury high-pressure arc lamps in housings equipped with quartz optics and dichroic mirrors in combination with cutoff filters (50% transmission at the wavelength specified). IR irradiation from the lamps was absorbed by a 10 cm path of water. A low pressure mercury arc lamp was used for 254 nm irradiation.

Computational Methods: Optimized geometries and vibrational frequencies of all species were calculated at the B3LYP level[14] employing the 6-311G(d,p) polarized valence-triple-ξ-basis set.[15] A spin-unrestricted formalism was used for all high-spin systems and for singlet biradicals, whenever an external instability[16] was observed. All DFT calculations were carried out with the Gaussian 03 suite of programs.[17] Computer simulation of the EPR spectra were performed by using the XSophe computer simulation software suite (version 1.0.4),[18] developed by the Centre for Magnetic Resonance and Department of Mathematics, University of Queensland, Brisbane (Australia) and Bruker Analytik GmbH, Rheinstetten (Germany).

Supporting Information (see footnote on the first page of this article): Additional figures and tables, and synthetic, spectroscopic and analytical data. Geometries, total energies and IR spectroscopic data of the photoproducts. Relative energies of all rearrangement products, and ^{1}H and ^{13}C NMR spectra.
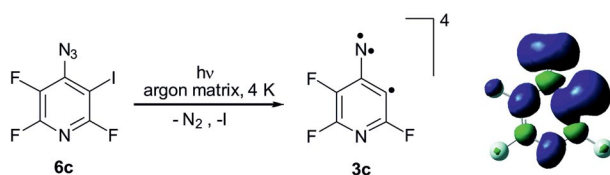
Acknowledgments

D. Grote, C. Finke, P. Neuhaus, W. Sander

[1] a) W. Sander, D. Grote, S. Kossmann, F. Neese, *J. Am. Chem. Soc.* **2008**, *130*, 4396–4403; b) H. Quast, W. Nudling, G. Klemm, A. Kirschfeld, P. Neuhaus, W. Sander, D. A. Hrovat, W. T. Borden, *J. Org. Chem.* **2008**, *73*, 4956–4961; c) K. Sato, D. Shiomi, T. Takui, M. Hattori, K. Hirai, H. Tomioka, *Mol. Cryst. Liq. Cryst. Sci. Technol. Sect. A* **2002**, *376*, 549–554; d) P. M. Lahti, *Magn. Prop. Org. Mater.* **1999**, 661–701.

[2] a) L. Catala, J. Le Moigne, N. Gruber, J. J. Novoa, P. Rabu, E. Belorizky, P. Turek, *Chem. Eur. J.* **2005**, *11*, 2440–2454; b) B. B. Wright, M. S. Platz, *J. Am. Chem. Soc.* **1983**, *105*, 628–630.

[3] P. Neuhaus, W. Sander, *Angew. Chem. Int. Ed.* **2010**, *49*, 7277–7280.

[4] P. Neuhaus, D. Grote, W. Sander, *J. Am. Chem. Soc.* **2008**, *130*, 2993–3000.

[5] a) P. M. Lahti, B. Esat, Y. Liao, P. Serwinski, J. Lan, R. Walton, *Polyhedron* **2001**, *20*, 1647–1652; b) P. Taylor, P. R. Serwinski, P. M. Lahti, *Org. Lett.* **2005**, *7*, 3693–3696; c) P. R. Serwinski, B. Esat, P. M. Lahti, Y. Liao, R. Walton, J. Lan, *J. Org. Chem.* **2004**, *69*, 5247–5260.

[6] H. F. Bettinger, W. Sander, *J. Am. Chem. Soc.* **2003**, *125*, 9726–9733.

[7] a) H. H. Wenk, W. Sander, *Angew. Chem.* **2002**, *114*, 2873; *Angew. Chem. Int. Ed.* **2002**, *41*, 2742–2745; b) D. Grote, W. Sander, *J. Org. Chem.* **2009**, *74*, 7370–7382; c) D. Grote, C. Finke, S. Kossmann, F. Neese, W. Sander, *Chem. Eur. J.* **2010**, *16*, 4496–4506.

[8] W. Sander, M. Winkler, B. Cakir, D. Grote, H. F. Bettinger, *J. Org. Chem.* **2007**, *72*, 715–724.

[9] a) N. P. Gritsan, M. S. Platz, *Chem. Rev.* **2006**, *106*, 3844–3867; b) J. C. Hayes, R. S. Sheridan, *J. Am. Chem. Soc.* **1990**, *112*, 5879–5881; c) W. T. Borden, N. P. Gritsan, C. M. Hadad, W. L. Karney, C. R. Kemnitz, M. S. Platz, *Acc. Chem. Res.* **2000**, *33*, 765–771; d) M. S. Platz, *Reactive Intermediate Chem.* (Eds.: R. A. Moss, M. S. Platz, M. Jones Jr,), Wiley, New York, **2004**, 501–559.

[10] a) R. Poe, K. Schnapp, M. J. T. Young, J. Grayzar, M. S. Platz, *J. Am. Chem. Soc.* **1992**, *114*, 5054–5067; b) K. A. Schnapp, M. S. Platz, *Bioconjugate Chem.* **1993**, *4*, 178–183; c) W. L. Karney, W. T. Borden, *J. Am. Chem. Soc.* **1997**, *119*, 3347–3350.

[11] J. Morawietz, W. Sander, *J. Org. Chem.* **1996**, *61*, 4351–4354.

[12] P. Fleischhauer, S. Gehring, C. Saal, W. Haase, Z. Tomkowicz, C. Zanchini, D. Gatteschi, D. Davidov, A. L. Barra, *J. Magn. Magn. Mater.* **1996**, *159*, 166–174.

[13] I. R. Dunkin, *Matrix Isolation Techniques: A Practical Approach*, Oxford University Press, Oxford, **1998**.

[14] a) A. D. Becke, *J. Chem. Phys.* **1993**, *98*, 5648–5652; b) C. Lee, W. Yang, R. G. Parr, *Phys. Rev. B* **1988**, *37*, 785–789.

[15] a) A. D. McLean, G. S. Chandler, *J. Chem. Phys.* **1980**, *72*, 5639–5648; b) R. Krishnan, J. S. Binkley, R. Seeger, J. A. Pople, *J. Chem. Phys.* **1980**, *72*, 650–654.

[16] R. Bauernschmitt, R. Ahlrichs, *J. Chem. Phys.* **1996**, *104*, 9047–9052.

[17] M. J. T. Frisch, G. W. Schlegel, H. B. Scuseria, G. E. M. A. Robb, J. R. Cheeseman, Montgomery Jr, J. A. T. Vreven, K. N. Kudin, J. C. Burant, J. M. Millam, S. S. Iyengar, J. Tomasi, V. Barone, B. Mennucci, M. Cossi, G. Scalmani, N. Rega, G. A. Petersson, H. Nakatsuji, M. Hada, M. Ehara, K. Toyota, R. Fukuda, J. Hasegawa, M. Ishida, T. Nakajima, Y. Honda, O. Kitao, H. Nakai, M. Klene, X. Li, J. E. Knox, H. P. Hratchian, J. B. Cross, V. Bakken, C. Adamo, J. Jaramillo, R. Gomperts, R. E. Stratmann, O. Yazyev, A. J. Austin, R. Cammi, C. Pomelli, J. W. Ochterski, P. Y. Ayala, K. Morokuma, G. A. Voth, P. Salvador, J. J. Dannenberg, V. G. Zakrzewski, S. Dapprich, A. D. Daniels, M. C. Strain, O. Farkas, D. K. Malick, A. D. Rabuck, K. Raghavachari, J. B. Foresman, J. V. Ortiz, Q. Cui, A. G. Baboul, S. Clifford, J. Cioslowski, B. B. Stefanov, G. Liu, A. Liashenko, P. Piskorz, I. Komaromi, R. L. Martin, D. J. Fox, T. Keith, M. A. Al-Laham, C. Y. Peng, A. Nanayakkara, M. Challacombe, P. M. W. Gill, B. Johnson, W. Chen, M. W. Wong, C. Gonzalez, and J. A. Pople, *Gaussian 03*, rev. C.02, Gaussian, Inc., Wallingford CT, **2004**.

[18] M. Griffin, A. Muys, C. Noble, D. Wang, C. Eldershaw, K. E. Gates, K. Burrage, G. R. Hanson, *Mol. Phys. Rep.* **1999**, *26*, 60–84.

EurJOC
European Journal
of Organic Chemistry

σ, σ, π - Triradical

D. Grote, C. Finke, P. Neuhaus,
W. Sander* **1–9**

The combination of an aryl radical with an arylnitrene results in new motives for the construction of organic high-spin molecules. Photolysis of 3-iodo-2,5,6-trifluoropyridyl azide under the conditions of matrix isolation results in the formation of a nitrene radical with a quartet ground state.

The electronic structure of this nitrene radical is described best as a σ,σ,π-triradical. The nitrene radical is stable at cryogenic temperatures but, upon irradiation, rearranges to a thermodynamically more stable azirinyl radical.